Published for SISSA by Springer

Received: *August 20, 2022*
Accepted: *August 26, 2022*
Published: *September 19, 2022*

Einstein-Gauss-Bonnet black strings at large α

Ryotaku Suzuki and Shinya Tomizawa

Mathematical Physics Laboratory Toyota Technological Institute,
Hisakata 2-12-1, Nagoya 468-8511, Japan

E-mail: sryotaku@toyota-ti.ac.jp, tomizawa@toyota-ti.ac.jp

Abstract: The simplest black string in higher-dimensional general relativity (GR) is perhaps the direct product of a Schwarzschild spacetime and a flat spatial direction. However, it is known that the Einstein-Gauss-Bonnet theory does not allow such a trivial and simple solution. We propose a novel analytic technique, which assumes that the Gauss-Bonnet (GB) term becomes dominant over the Einstein-Hilbert (EH) term. Assuming the dimensionless coupling constant α normalized by the horizon scale is large enough, we find that the spacetime is separated into the GB region and GR region, which are matched via the transition region where the GB and EH terms are comparable. Using this *large* α *approximation*, we indeed construct new analytic solutions of black strings, from which we analytically compute various physical quantities of black strings at large α. Moreover, we confirm that all these analytic results are consistent with the numerical calculation. We also discuss the possible extension to general Einstein-Lovelock black holes.

Keywords: Black Holes, Black Holes in String Theory, Classical Theories of Gravity

ArXiv ePrint: 2208.02497

Open Access, © The Authors.
Article funded by SCOAP[3].

https://doi.org/10.1007/JHEP09(2022)135

JHEP09(2022)135

Contents

JHEP09(2022)135

1 Introduction

For two decades, black holes in dimensions more than four have attracted many physicists from a point of view of scientific and applied researches, for instance, by the microscopic derivation of Bekenstein-Hawking entropy [1], the realistic production of black holes at accelerators in the scenario of large extra dimensions [2], and AdS/CFT correspondence [3]. The recent developments by many researchers show the richness of such solutions and the

complexity of the dynamics [4]. In particular, a black string is one of the simplest non-spherical black objects which can be constructed by simply adding a flat spatial direction to the Schwarzschild-Tangherlini black hole [5]. For simplicity, it has been a major testing ground for the black hole dynamics proper to higher dimensional black holes such as the Gregory-Laflamme instability [6, 7].

So far, higher-dimensional black holes are studied mostly in Einstein's theory of general relativity (GR). However, GR is not a unique theory of gravity in higher dimensions, but it can also include higher curvature corrections, which are inspired from the string theory in the ultraviolet scale [8]. Einstein-Lovelock theories are one of such generalization of GR to the higher curvature theories whose equations of motion are second order differential equations. It is of great interest in theoretical physics as it describes a wide class of models. In Einstein-Lovelock theories, the only found exact solutions of black holes are static and spherically symmetric black hole solutions due to the lack of analytical methods. Moreover, even black string solutions cannot be obtained by the simple addition of a flat spatial direction [9]. However, it is known that black strings admit such simple construction in the pure Lovelock theories that only have a single Lovelock term without Einstein-Hilbert (EH) term in the action [10, 11]. The inclusion of the negative cosmological constant and supporting scalar or p-form fields also admits another types of homogeneous Einstein-Lovelock black branes [12–15], which are hinted by the construction of homogeneous AdS black branes supported by scalar fields [16].

In this article, we focus on the d (> 4)-dimensional Einstein-Lovelock theory with only quadratic curvature corrections, i.e., the d-dimensional Einstein-Gauss-Bonnet (EGB) theory, whose action is given by

$$S = \frac{1}{16\pi G}\int d^d x\sqrt{-g}(R + \alpha_{\rm GB}\mathcal{L}_{\rm GB}), \tag{1.1}$$

where the Gauss-Bonnet (GB) term is written as

$$\mathcal{L}_{\rm GB} := R^2 - 4R_{\mu\nu}R^{\mu\nu} + R_{\mu\nu\rho\sigma}R^{\mu\nu\rho\sigma}. \tag{1.2}$$

In the EGB theory, a fundamental parameter of the theory is the coupling constant $\alpha_{\rm GB}$. Hence it might be natural to study to construct black strings for small coupling constant [17–19]. This limit is also used for the construction of spinning black holes in the five-dimentional EGB theory [20]. Another controllable parameter is the dimension d, which leads to the large d limit [21, 22] that is also useful in the construction of EGB black strings [23, 24] and EGB rotating black holes [25]. Besides these limiting solutions, EGB black string solutions were numerically obtained as well [17–19].

Now let us consider another new possibility of the parameter limit, in which the GB term becomes dominant over the EH term around black holes or certain compact objects

$$R \ll \alpha_{\rm GB}\mathcal{L}_{\rm GB}. \tag{1.3}$$

This leads us to an interesting approximation, which we call *the large α approximation*, where α is the dimensionless coupling constant normalized by the spacetime curvature

JHEP09(2022)135

around the system $R \sim \mathcal{R}$,[1]

$$\alpha \sim \alpha_{\rm GB}\mathcal{R} \gg 1. \tag{1.4}$$

For black holes of the radius r_0, it should simply be $\mathcal{R} \sim 1/r_0^2$, and hence, one can also interpret this as the large curvature approximation or small black hole approximation when $\alpha_{\rm GB}$ is fixed. At the limit $\alpha \to \infty$, it is natural to expect that spacetime geometry approaches that of the pure GB theory, in which black strings restore a simple construction with a flat spatial direction [10, 11]. Indeed, static EGB black holes approach static pure GB black holes at large α [26]. The big difference from the pure GB theory is that arbitrarily large but finite α causes the breakdown of the assumption (1.3) near the flat region where the spacetime becomes almost GR

$$R \gg \alpha_{\rm GB}\mathcal{L}_{\rm GB}. \tag{1.5}$$

In our previous study on the stable bound orbits around the spherical EGB black hole [27], we found that these two regions, which from now on we call *the GB region* and *the GR region*, can be matched by an intermediate region of the *transition region*. In this article, we use the large α approximation to construct EGB black strings. More precisely, we solve the EGB equations in the GB, transition and GR region analytically, and then match them to obtain the entire geometry. The physical quantities are also derived up to the leading order and compared with the numerical calculation in $d = 6, \ldots, 10$. To see the validity of the large α approximation, we confirm whether the analytical result fits well with the numerical result in the large α regime.

The rest of this article is organized as follows. We first explain the setup in section 2. In section 3, we revisit EGB black holes at large α. Then, the GB region of EGB black strings is solved at large α in section 4. In section 5, we study the matching in the transition region to connect the metric in the GB region and asymptotically flat background, and then obtain the expression for the physical quantities. These analytic results are compared with the numerical calculation in section 6. Finally, we discuss the possible extension to Einstein-Lovelock black holes in section 7. The results are summarized in section 8.

2 Setup

From the action (1.1), the EGB equation can be derived as

$$R_{\mu\nu} - \frac{1}{2}Rg_{\mu\nu} + \alpha_{\rm GB}H_{\mu\nu} = 0 \tag{2.1}$$

where $H_{\mu\nu}$ is the Lanzcoz tensor given by

$$H_{\mu\nu} = 2RR_{\mu\nu} - 4R_{\mu\alpha}R^{\alpha}{}_{\nu} - 4R_{\mu\alpha\nu\beta}R^{\alpha\beta} + 2R_{\mu\alpha\beta\gamma}R_{\nu}{}^{\alpha\beta\gamma} - \frac{1}{2}\mathcal{L}_{\rm GB}g_{\mu\nu}. \tag{2.2}$$

[1] We only consider the positive $\alpha_{\rm GB}$, since the coupling constant is bound below in the negative case.

JHEP09(2022)135

Let us consider a $d = n + 4$ uniform black string under the ansatz following the convention in ref. [18]

$$ds^2 = -b(r)dt^2 + \frac{dr^2}{f(r)} + a(r)dz^2 + r^2 d\Omega_{n+1}^2. \tag{2.3}$$

We assume that the metric asymptotes to the Kaluza-Klein background $M_{n+3} \times S^1$, i.e., the direct product of a $(n + 3)$-dimensional Minkowski spacetime and a flat compact direction, which can be written at $r \to \infty$ as

$$a \to 1, \quad b \to 1, \quad f \to 1, \tag{2.4}$$

with z-direction identified by $z \sim z + L$. The asymptotic behavior to this background is solved as

$$b = 1 - \frac{c_t}{r^n}, \quad a = 1 + \frac{c_z}{r^n}, \quad f = 1 - \frac{c_t - c_z}{r^n}. \tag{2.5}$$

This enables us to determine the mass M and tension $\mathcal{T}$ by using the Arnowitt-Deser-Misner (ADM) formula in [28],

$$M = \frac{\Omega_{n+1} L}{16\pi G}((n+1)c_t - c_z), \quad \mathcal{T} = \frac{\Omega_{n+1}}{16\pi G}(c_t - (n+1)c_z). \tag{2.6}$$

The so-called relative tension, or relative binding energy, is also computed as

$$N = \frac{\mathcal{T} L}{M} = \frac{c_t - (n+1)c_z}{(n+1)c_t - c_z}. \tag{2.7}$$

The Hawking temperature $T_{\rm H}$ is defined by the surface gravity

$$T_{\rm H} = \frac{\kappa}{2\pi} = \frac{1}{4\pi r_0}\sqrt{f'(r_0)a'(r_0)}, \tag{2.8}$$

where $r = r_0$ is the horizon radius. Moreover, the black hole entropy can be derived by the Iyer-Wald formula [29, 30] as

$$S = \frac{1}{4G}\int_H (1 + 2\alpha_{\rm GB}\mathcal{R})\, dS = \frac{\Omega_{n+1}}{4G} r_0^{n+1}\left(1 + \frac{2n(n+1)\alpha_{\rm GB}}{r_0^2}\right)\sqrt{a(r_0)} \tag{2.9}$$

where $\mathcal{R}$ is the spatial curvature on the horizon.

3 EGB black holes at large α

In our previous study on stable bound orbits around the spherical EGB black holes [31], we have found that the large α approximation provides us a useful analytic approach, which simplifies the analysis of the geodesic motion [27]. Before the black string analysis, we revisit the large α limit for asymptotically flat, static and spherically symmetric EGB black holes in the $(n + 3)$-dimension. The metric of the EGB black hole spacetime is given by

$$ds^2 = -F(r)dt^2 + \frac{dr^2}{F(r)} + r^2 d\Omega_{n+1}^2, \tag{3.1}$$

JHEP09(2022)135

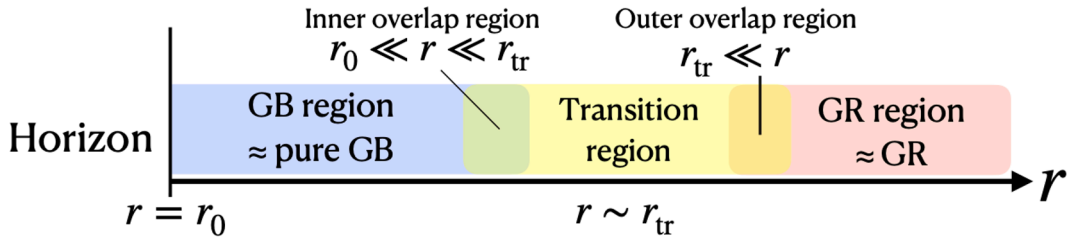

Figure 1. Two separate regions in EGB black holes at large α.

with

$$F(r) = 1 + \frac{r^2}{2\alpha r_0^2}\left(1 - \sqrt{1 + \frac{4\alpha(\alpha+1)r_0^{n+2}}{r^{n+2}}}\right), \tag{3.2}$$

where the horizon is at $r = r_0$, and we have introduced the dimensionless coupling constant by

$$\alpha := \frac{n(n-1)\alpha_{\rm GB}}{r_0^2}. \tag{3.3}$$

In ref. [26], it is noticed that this solution is endowed with the following two regimes. For the large α with fixed r, the solution approaches a black hole spacetime in the pure GB theory

$$F(r) \simeq 1 - \left(\frac{r_0}{r}\right)^{\frac{n-2}{2}}. \tag{3.4}$$

On the other hand, the limit $r \to \infty$ with fixed α recovers the asymptotic behavior in $d = n + 3$ GR

$$F(r) \simeq 1 - \frac{(\alpha+1)r_0^n}{r^n}. \tag{3.5}$$

In ref. [27], it is further pointed out that two regions, where we call the GB region and the GR region, are separated by the transition scale

$$r_{\rm tr} = r_0\, \alpha^{\frac{2}{n+2}}, \tag{3.6}$$

which can be seen from figure 1. Around this scale $r \sim r_{\rm tr}$ a transition region is formed, which has sufficient overlaps with other two regions to allow the matched asymptotic expansion. For $n = 2$ ($d = 5$), the pure GB theory becomes kinematic as the three dimensional GR, and there is no black hole solution without negative cosmological constant [32, 33]. Nevertheless, eq. (3.2) still admits a horizon in the large α approximation for $n = 2$

$$F(r) \simeq \frac{r^2 - r_0^2}{2\alpha r_0^2}. \tag{3.7}$$

Unlike $n > 2$ cases, we cannot take the limit $\alpha \to \infty$ in $F(r)$. Taking into account such difference, we consider $n > 2$ cases and $n = 2$ separately in the following analysis.

JHEP09(2022)135

4 EGB black strings in GB region

First, we consider the GB region. Although a simple direct product of the $(n+3)$-dimensional black hole metric (3.1) with a one-dimensional flat metric is not a solution to the $(n+4)$-dimensional EGB equation (2.1), we expect that the spatial section of a $(n+4)$-dimensional black string (2.3) has the same separation of scales as the $(n+3)$-dimensional black hole in the transverse direction. Note that we consider only $n \geq 2$ ($d \geq 6$) since for $n = 1$ ($d = 5$) $\alpha_{\rm GB}$ is bounded above by the horizon scale [17],[2] and hence our approach cannot be used. We introduce the dimensionless constant α by eq. (3.3) in which the black hole radius is replaced with the black string radius. In the following, as mentioned in the previous section, we study the $n > 2$ cases and $n = 2$ case separately by using the $1/\alpha$ expansion.

4.1 $n > 2$ cases

For $n > 2$, the black string solution for the pure GB theory is easily found as [10]

$$b(r) = f(r) = 1 - \left(\frac{r_0}{r}\right)^{\frac{n-2}{2}}, \quad a(r) = 1, \tag{4.1}$$

where we set the horizon at $r = r_0$. Then, we consider the $1/\alpha$-correction

$$b = b_H\left(1 - \left(\frac{r_0}{r}\right)^{\frac{n-2}{2}} + \frac{1}{\alpha}b_1\right), \quad f = 1 - \left(\frac{r_0}{r}\right)^{\frac{n-2}{2}} + \frac{1}{\alpha}f_1, \quad a = a_H\left(1 + \frac{1}{\alpha}a_1\right) \tag{4.2}$$

where b_H and a_H are the constant scales of t and z, which are determined by the asymptotic behavior. From the combination of some equations of motion (see appendix A.1), the equations for a_1, b_1 and f_1 are written as, respectively,

$$\frac{d}{dr}\left[r\left(\left(\frac{r}{r_0}\right)^{\frac{n-2}{2}} - 1\right)\frac{d}{dr}a_1\right] = \frac{n+4}{2n(n+1)r_0}\left(\frac{r}{r_0}\right)^{\frac{n}{2}}, \tag{4.3}$$

$$\begin{aligned}\partial_r\left(\frac{b_1}{1-(r/r_0)^{-\frac{n-2}{2}}}\right) &= \frac{2n-(n+2)(r/r_0)^{-\frac{n-2}{2}}}{4(n-1)\left(1-(r/r_0)^{-\frac{n-2}{2}}\right)}a_1' \\ &\quad - \frac{(n-2)f_1}{2r\left(1-(r/r_0)^{-\frac{n-2}{2}}\right)^2} + \frac{(n+2)r}{4(n-1)nr_0^2\left(1-(r/r_0)^{-\frac{n-2}{2}}\right)},\end{aligned} \tag{4.4}$$

$$f_1 = \frac{(n-2)(n+3)(r/r_0)^2}{2n(n+2)(n^2-1)} + \frac{C_1}{r^{\frac{n-2}{2}}} + \frac{n-2}{4(n-1)}\left(\frac{r_0}{r}\right)^{\frac{n-2}{2}}a_1, \tag{4.5}$$

where C_1 is an integration constant. The regular solution of eq. (4.3) becomes

$$a_1 = \frac{2(n+4)}{(n-2)n(n+1)(n+2)}\mathsf{F}_n\left((r_0/r)^{\frac{n-2}{2}}\right), \tag{4.6}$$

where we defined

$$\mathsf{F}_n(x) := \int_x^1 \frac{y^{\frac{n+2}{2-n}} - 1}{1-y}dy. \tag{4.7}$$

[2] Interestingly, ref. [34] investigates black strings close to the maximum $\alpha_{\rm GB,max}$ in five dimension.

JHEP09(2022)135

Then, f_1 and b_1 are solved as, respectively,

$$b_1 = \frac{(r/r_0)^2-1}{2n(n-1)} - \frac{8+5n}{2n(n-2)(n^2-1)}\left(1-\left(\frac{r_0}{r}\right)^{\frac{n-2}{2}}\right) - \frac{(n+4)\left(4-(n+2)(r_0/r)^{\frac{n-2}{2}}\right)\mathsf{F}_n\left((r_0/r)^{\frac{n-2}{2}}\right)}{2n(n^2-1)(n^2-4)}, \tag{4.8}$$

$$f_1 = \frac{(n-2)(n+3)r^2}{2n(n+2)(n^2-1)r_0^2} - \frac{(n-2)(n-3)-(n+4)\mathsf{F}_n\left((r_0/r)^{\frac{n-2}{2}}\right)}{2n(n^2-1)(n+2)}\left(\frac{r_0}{r}\right)^{\frac{n-2}{2}}, \tag{4.9}$$

where the integration constants are determined by $b_1(r_0) = b_1'(r_0) = f_1(r_0) = a_1(r_0) = 0$. All the scaling degrees of freedom for $t \to \lambda_1 t$ and $z \to \lambda_2 z$ are absorbed into a_H and b_H.

4.2 $n = 2$ case

In the $n = 2$ case, the black hole result (3.7) suggests that the metric function should scale as $f = \mathcal{O}(\alpha^{-1})$. This rescaling actually leads to the leading order solution at large α

$$a = a_H \frac{r^2}{r_0^2}, \quad f = \frac{1}{6\alpha}\left(\frac{r^2}{r_0^2} - \frac{r_0}{r}\right), \quad b = b_H\left(\frac{r^2}{r_0^2} - \frac{r_0}{r}\right), \tag{4.10}$$

where a_H and b_H are again the scaling constant of z and t. Clearly, this leading order metric cannot have asymptotically flat region at $r \to \infty$, but rather tends to be a warped product of AdS_3 and S^3,

$$ds^2 \simeq 6\alpha r_0^2\left[\frac{dr^2}{r^2} + \frac{r^2}{r_0^2}\left(-d\bar{t}^2 + d\bar{z}^2\right)\right] + r^2 d\Omega_3^2, \quad \bar{t} := \sqrt{\frac{b_H}{6\alpha}}\frac{t}{r_0}, \quad \bar{z} := \sqrt{\frac{a_H}{6\alpha}}\frac{t}{r_0}. \tag{4.11}$$

The $1/\alpha$ correction

$$a = a_H\left(\frac{r^2}{r_0^2} + \frac{a_1}{\alpha}\right), \quad f = \frac{1}{6\alpha}\left(\frac{r^2}{r_0^2} - \frac{r_0}{r}\right) + \frac{f_1}{\alpha^2}, \quad b = b_H\left(\frac{r^2}{r_0^2} - \frac{r_0}{r} + \frac{b_1}{\alpha}\right), \tag{4.12}$$

is easily found as

$$a_1 = \frac{r}{2r_0}\,{}_2F_1\left(\frac{1}{3}, 1, \frac{4}{3}; \frac{r_0^3}{r^3}\right) - \frac{r(r^3+r_0^3)}{6r_0^4} + \frac{r^2}{6r_0^2}\log\left(1-\frac{r_0^3}{r^3}\right), \tag{4.13a}$$

$$b_1 = \frac{(H_{1/3}-1)r_0}{24r} + \frac{(2r^3+r_0^3)^2}{24rr_0^5}\,{}_2F_1\left(\frac{1}{3}, 1, \frac{4}{3}; \frac{r_0^3}{r^3}\right)\log\left(1-\frac{r_0^3}{r^3}\right) - \frac{4r^6+3r_0^3r^3-r_0^6}{72r^2r_0^4}, \tag{4.13b}$$

$$f_1 = \frac{(H_{1/3}-1)r_0}{24r} + \frac{r_0^2}{8r^2}\,{}_2F_1\left(\frac{1}{3}, 1, \frac{4}{3}; \frac{r_0^3}{r^3}\right) + \frac{r(2r^3-3r_0^3)}{72r_0^4} + \frac{r_0}{24r}\log\left(1-\frac{r_0^3}{r^3}\right) - \frac{(6r-r_0)r_0}{72r^2}. \tag{4.13c}$$

where ${}_2F_1(a, b, c; x)$ is the hypergeometric function.

JHEP09(2022)135

5 Transition region

Since the GB-dominant condition (1.3) breaks down near the flat region, the previous GB-dominant solution in the large α approximation needs a continuation to the asymptotically flat region through the transition region around $r \sim r_{\rm tr} = r_0 \alpha^{\frac{2}{n+2}}$, in which we will use the rescaled coordinate

$$u := r/r_{\rm tr}. \tag{5.1}$$

The solution in the transition region is matched with the GB-dominant solution in the inner overlap region ($r_0 \ll r \ll r_{\rm tr}$ or $u \ll 1$) and with the asymptotic solution (2.5) in the outer overlap region ($r \gg r_{\rm tr}$ or $u \gg 1$), respectively. As in the GB region, the $n > 2$ cases and $n = 2$ case are studied separately.

5.1 $n > 2$

First, we consider the behavior of the GB-dominant solution in the inner overlap region in terms of the rescaled coordinate (5.1), in which the leading order solution (4.6) behaves as

$$b/b_H \simeq f \simeq 1 - \left(\frac{r_0}{r}\right)^{\frac{n-2}{2}} = 1 - \alpha^{-\frac{n-2}{n+2}} u^{-\frac{n-2}{2}}. \tag{5.2}$$

From eq. (B.7), the next-to-leading order correction (4.6), (4.8), (4.9) behaves as the same order,

$$\frac{a_1}{\alpha} \sim \frac{b_1}{\alpha} \sim \frac{f_1}{\alpha} \sim \frac{r^2}{\alpha} = \alpha^{-\frac{n-2}{n+2}} u^2. \tag{5.3}$$

Therefore, we expect the metric functions in the transition region to take the following form

$$a = a_H \left(1 + \alpha^{-\frac{n-2}{n+2}} A(u)\right), \quad b = b_H \left(1 + \alpha^{-\frac{n-2}{n+2}} B(u)\right), \quad f = 1 + \alpha^{-\frac{n-2}{n+2}} F(u), \tag{5.4}$$

where $A(u), B(u), F(u)$ are regular functions of u, which satisfy

$$A(u) \simeq \text{const.}, \quad B(u) \simeq -u^{-\frac{n-2}{2}}, \quad F(u) \simeq -u^{-\frac{n-2}{2}} \quad \text{for} \quad u \ll 1. \tag{5.5}$$

From the behavior of the metric (5.4), one can expect a certain simplification by expanding the EGB equation (A.1) in the power of $\alpha^{-\frac{n-2}{n+2}}$. Note that the same power $\alpha^{-\frac{n-2}{n+2}}$ also appears in the effective potential of the EGB black holes [27]. We can notice that eqs. (A.1a) and (A.1b) to the leading order in $\alpha^{-\frac{n-2}{n+2}}$ are integrable to give

$$A'(u) = \frac{(n^2-1)u^{-n-1}\left(\alpha_1 u^2 + u^{n+2}F(u) - u^n F(u)^2\right)}{2(n+1)F(u) - (n-1)u^2}, \tag{5.6}$$

$$B'(u) = \frac{(n^2-1)u^{-n-1}\left(\beta_1 u^2 + u^{n+2}F(u) - u^n F(u)^2\right)}{2(n+1)F(u) - (n-1)u^2}, \tag{5.7}$$

where α_1, β_1 is integration constants. Using the above equations, and eliminating $A'(u)$ and $B'(u)$ from the leading order of eq. (A.1c), we obtain the quartic equation with respect

JHEP09(2022)135

to $F(u)$

$$\begin{aligned}
&\left(n^2-1\right)u^8\left(2\alpha_1\beta_1\,(n+1)\,u^{-2n-4}+(n-1)(\alpha_1+\beta_1)u^{-n-2}\right)\\
&-(n-1)^2u^6\left(2(\alpha_1+\beta_1)(n+1)u^{-n-2}-n-2\right)F(u)\\
&+(n-1)u^4\left(2(\alpha_1+\beta_1)(n+1)^2u^{-n-2}-3(n-1)(n+2)\right)F(u)^2\\
&+4(n^2-3)(n+1)u^2F(u)^3-2(n+1)^3F(u)^4=0.
\end{aligned}\tag{5.8}$$

If we introduce the function $\tilde{F}(u)$ and the variable x by

$$\tilde{F}:=F/u^2,\quad x:=u^{-n-2}.\tag{5.9}$$

Eq. (5.8) reduces to the quadratic equation with respect to x as

$$\begin{aligned}
&\tilde{F}(x)\left(-2(n+1)^3\tilde{F}(x)^3+4(n+1)(n^2-3)\tilde{F}(x)^2-3(n-1)^2(n+2)\tilde{F}(x)+(n-1)^2(n+2)\right)\\
&+\left(n^2-1\right)(\alpha_1+\beta_1)\left(2\,(n+1)\,\tilde{F}(x)^2-2(n-1)\tilde{F}(x)+n-1\right)x+2\alpha_1\beta_1\,(n-1)\,(n+1)^2x^2=0,
\end{aligned}\tag{5.10}$$

which admits two branches

$$x=\frac{1}{4(n-1)(n+1)^2(n^2-1)\alpha_1\beta_1}\left[-(\alpha_1+\beta_1)(2(n+1)n^2\tilde{F}^2-2(n-1)\tilde{F}-n+1)\pm\sqrt{Q(\tilde{F})}\right],\tag{5.11}$$

where

$$\begin{aligned}
Q(\tilde{F})=&\,4(n-1)(n+1)^4\left(2(3n+1)\alpha_1\beta_1+(n-1)(\alpha_1^2+\beta_1^2)\right)\tilde{F}^4\\
&-8(n+1)^3(n-1)\left(2(n+1)(3n-5)\alpha_1\beta_1+(n-1)^2(\alpha_1^2+\beta_1^2)\right)\tilde{F}^3\\
&+8(n+1)^2(n-1)^3\left((5n+6)\alpha_1\beta_1+n\left(\alpha_1^2+\beta_1^2\right)\right)\tilde{F}^2\\
&+4(n+1)^2(n-1)^3\left((\alpha_1-\beta_1)^2-n\left(4\alpha_1\beta_1+\alpha_1^2+\beta_1^2\right)\right)\tilde{F}+(n-1)^4(n+1)^2\,(\alpha_1+\beta_1)^2.
\end{aligned}\tag{5.12}$$

5.1.1 Matching in the inner overlap region $r_0 \ll r \ll r_{\rm tr}$ ($u \ll 1$)

Now, we consider the matching between the GB region, which has an overlap with the transition region for $r_0 \ll r \ll r_{\rm tr}$ ($u \ll 1$). The matching condition (5.5) requires

$$\tilde{F}\simeq -u^{-\frac{n+2}{2}}=-\sqrt{x}\quad\text{for}\quad x\ll 1..\tag{5.13}$$

One the other hand, expanding eq. (5.11) for $|\tilde{F}|\gg 1$, we obtain

$$x\simeq\frac{-(n-1)(\alpha_1+\beta_1)\pm\sqrt{(n-1)((n-1)(\alpha_1^2+\beta_1^2)+2(3n+1)\alpha_1\beta_1)}}{2(n-1)\alpha_1\beta_1}\tilde{F}^2+\mathcal{O}(\tilde{F}),\tag{5.14}$$

JHEP09(2022)135

yielding a matching condition

$$1 = -\frac{2(n-1)\alpha_1\beta_1}{(n-1)(\alpha_1+\beta_1) \pm \sqrt{(n-1)((n-1)(\alpha_1^2+\beta_1^2)+2(3n+1)\alpha_1\beta_1)}}. \tag{5.15}$$

Plugging the behavior of $F(u)$ in eq. (5.5) into eqs. (5.6) and (5.7), we obtain A and B for $u \ll 1$,

$$A \simeq \text{const.} + \frac{(n-1)(\alpha_1-1)}{n-2} u^{-\frac{n-2}{2}}, \quad B \simeq \text{const.} + \frac{(n-1)(\beta_1-1)}{n-2} u^{-\frac{n-2}{2}}. \tag{5.16}$$

Comparing this with $A(u)$ and $B(u)$ in eq. (5.5), we can determine

$$\alpha_1 = 1, \quad \beta_1 = \frac{1}{n-1}. \tag{5.17}$$

It is easy to check that this condition also satisfies eq. (5.15).

5.1.2 Matching in the outer overlap region $r \gg r_{\rm tr}$ ($u \gg 1$)

In the outer overlap region $r \gg r_{\rm tr}$ ($u \gg 1$), matching with the asymptotically flat background $f \to 1$ requires $\tilde{F} \simeq 0$ for $x \ll 1$. Expanding eq. (5.11) around $\tilde{F} \simeq 0$, we obtain

$$x \simeq \frac{n-1}{4(n+1)\alpha_1\beta_1}(-\alpha_1-\beta_1 \pm |\alpha_1+\beta_1|) + \mathcal{O}(\tilde{F}). \tag{5.18}$$

Therefore, for the consistent match, we should choose (+) branch because $\alpha_1+\beta_1 = n/(n-1) > 0$, that gives

$$x = \frac{1}{4n^2(n^2-1)}\left[-n(2n^2(n^2-1)\tilde{F}^2 - 2n(n-1)\tilde{F}+1) + \sqrt{\tilde{Q}(\tilde{F})}\right] \tag{5.19}$$

with

$$\begin{aligned}\tilde{Q}(\tilde{F}) = {}& 4n^4(n^2-1)^2(n+2)^2\tilde{F}^4 - 8n^3(n^2-1)(n^3+3n^2-12)\tilde{F}^3 \\ & + 8n^2(n-1)(n^3+3n^2+3n-6)\tilde{F}^2 - 4n(n-1)(n^2+2n+4)\tilde{F} + n^2.\end{aligned} \tag{5.20}$$

Finally, from eq. (5.19), we can determine the behavior of F in the outer overlap region $r \gg r_{\rm tr}$ ($u \gg 1$) as

$$F \simeq -\frac{n(n+1)}{(n-1)(n+2)}\frac{1}{u^n}, \tag{5.21}$$

which also determines the behavior of A and B through eqs. (5.6) and (5.7),

$$A \simeq \text{const.} - \frac{2(n+1)}{n(n-1)(n+2)}\frac{1}{u^n}, \quad B \simeq \text{const.} - \frac{(n+1)(n^2-2)}{n(n-1)(n+2)}\frac{1}{u^n} \tag{5.22}$$

From the original form (5.4), the metric functions behave as

$$a \simeq a_H\left(1 + \text{const.} \times \alpha^{-\frac{n-2}{n+2}}\right) - \frac{2(n+1)\alpha\, a_H}{n(n-1)(n+2)}\frac{r_0^n}{r^n}, \tag{5.23a}$$

$$b \simeq b_H\left(1 + \text{const.} \times \alpha^{-\frac{n-2}{n+2}}\right) - \frac{(n+1)(n^2-2)\alpha\, b_H}{n(n-1)(n+2)}\frac{r_0^n}{r^n}. \tag{5.23b}$$

JHEP09(2022)135

The scaling constants need $\mathcal{O}(\alpha^{-\frac{n-2}{n+2}})$ corrections so that the metric asymptotes to the Minkowski at $r \to \infty$,

$$a_H = 1 + \mathcal{O}(\alpha^{-\frac{n-2}{n+2}}), \quad b_H = 1 + \mathcal{O}(\alpha^{-\frac{n-2}{n+2}}). \tag{5.24}$$

From the ADM formula (2.6), eq. (5.23) leads to the mass and tension at large α

$$M \simeq \frac{(n+1)\Omega_{n+1}}{16\pi G}\alpha\, r_0^n L, \tag{5.25}$$

$$\mathcal{T} \simeq \frac{(n+1)\Omega_{n+1}}{16\pi G(n-1)}\alpha\, r_0^n. \tag{5.26}$$

Particularly, the relative tension approaches a finite limit at large α

$$N = \frac{L\mathcal{T}}{M} \simeq \frac{1}{n-1}, \tag{5.27}$$

which is greater than that of the black string in GR

$$N_{\rm GR} = \frac{1}{n+1}. \tag{5.28}$$

Since the scaling constants are determined as $a_H \simeq b_H \simeq 1$, the temperature and entropy are identical to that of the pure Gauss-Bonnet metric (4.1) at the leading order

$$T_{\rm H} \simeq \frac{n-2}{8\pi}\frac{1}{r_0}, \tag{5.29}$$

$$S \simeq \frac{(n+1)\Omega_{n+1}}{2G(n-1)}\alpha\, r_0^{n+1} L. \tag{5.30}$$

It is easy to verify that these variables satisfy the first law with the variation of (r_0, L) at $\mathcal{O}(\alpha)$

$$dM = T_{\rm H} dS + \mathcal{T} dL, \tag{5.31}$$

and the Smarr-type formula (A.4) [18]

$$M = \mathcal{T} L + T_{\rm H} S. \tag{5.32}$$

Note that the matching result (5.24) shows that the corrections to these variables should be given in the power of $\alpha^{-\frac{n-2}{n+2}}$, or both of $\alpha^{-\frac{n-2}{n+2}}$ and α^{-1}, rather than the simple expansion in α^{-1}. However, we will not pursue determining the correction terms, as it will require more laborious calculations.

JHEP09(2022)135

5.1.3 Fragmentation at large α

As we obtained the mass and entropy of the black string of the length L at large α, let us compare the entropy with that of the black hole of the same mass. The mass and entropy of the $d = n + 4$ Boulware-Deser black hole with the radius r_H is given by

$$M_{\rm BH} = \frac{(n+2)\Omega_{n+2}}{16\pi G}\left(n(n+1)\alpha_{\rm GB} + r_H^2\right) r_H^{n-1} \simeq \frac{(n+1)(n+2)\Omega_{n+2}}{16\pi G(n-1)}\alpha\, r_0^2\, r_H^{n-1} \tag{5.33}$$

and

$$S_{\rm BH} = \frac{\Omega_{n+2}}{4G}\left(1 + \frac{2(n+1)(n+2)\alpha_{\rm GB}}{r_H^2}\right) r_H^{n+2} \simeq \frac{(n+1)(n+2)\Omega_{n+2}}{2Gn(n-1)}\alpha\, r_0^2\, r_H^{n}, \tag{5.34}$$

where eq. (3.3) is used. Comparing with eq. (5.25), the corresponding black hole radius is given by

$$r_H = \left(\frac{(n-1)\Omega_{n+1}}{(n+2)\Omega_{n+2}}\right)^{\frac{1}{n-1}} r_0^{\frac{n-2}{n-1}} L^{\frac{1}{n-1}}. \tag{5.35}$$

Therefore, using eq. (5.30), the entropy ratio becomes

$$\frac{S}{S_{\rm BH}} \simeq \frac{n\Omega_{n+1}}{(n+2)\Omega_{n+2}}\frac{r_0^{n-1}L}{r_H^n} = C\left(\frac{r_0}{L}\right)^{\frac{1}{n-1}}, \quad C := \frac{n}{n-1}\left(\frac{(n+2)\Omega_{n+2}}{(n-1)\Omega_{n+1}}\right)^{\frac{1}{n-1}} \tag{5.36}$$

This ensures that the black hole phase has larger entropy, and hence the Gregory-Laflamme instability occurs for thin enough strings $r_0 \ll L$ even at the large α limit, which is in accordance with the fact that pure GB black strings are dynamically unstable [26].

5.2 $n = 2$

From the GB-dominant solution in eqs. (4.10) and (4.13), the behavior in the inner overlap region $r_0 \ll r \ll r_{\rm tr}$ ($u \ll 1$) is given by

$$a \simeq a_H\alpha\left(u^2 - \frac{u^4}{6}\right), \quad b \simeq b_H\alpha\left(u^2 - \frac{u^4}{18}\right), \quad f \simeq \frac{u^2}{6} + \frac{u^4}{36}. \tag{5.37}$$

This suggests the metric functions should take the following form in the transition region

$$a = a_H\alpha\,\bar{A}(u), \quad b = b_H\alpha\,\bar{B}(u), \quad f = \bar{F}(u), \tag{5.38}$$

where $\bar{A}(u), \bar{B}(u)$ and $\bar{F}(u)$ are regular functions of u. Unfortunately, unlike the $n > 2$ cases, this ansatz never simplifies the EGB equation (A.1) in the transition region, since all the terms become comparable as functions of u. However, we can still estimate the behavior in the outer overlap region as

$$\bar{A}(u), \bar{B}(u), \bar{F}(u) \simeq \text{const.} + \frac{\text{const.}}{u^2}, \quad \text{for} \quad u \gg 1. \tag{5.39}$$

JHEP09(2022)135

Therefore, the asymptotic behavior of metric functions become

$$a = a_H \alpha \left(\text{const.} + \text{const.} u^{-2}\right) = 1 + \text{const.} \frac{\alpha}{r^2} \tag{5.40}$$

$$b = b_H \alpha \left(\text{const.} + \text{const.} u^{-2}\right) = 1 + \text{const.} \frac{\alpha}{r^2}, \tag{5.41}$$

where the scaling constants are set as $a_H, b_H \sim \alpha^{-1}$ so that the Minkowski background is recovered at $r \to \infty$. This estimates the large α behavior of each variables

$$M \sim \alpha, \quad \mathcal{T} \sim \alpha, \quad T_{\rm H} \sim \sqrt{b_H \alpha^{-1}} \sim \frac{1}{\alpha}, \quad S \sim \alpha \sqrt{a_H} \sim \sqrt{\alpha}. \tag{5.42}$$

Using the Smarr formula $N = 1 - T_{\rm H} S/M$, one can also estimate the behavior of the relative tension as

$$N = 1 - \mathcal{O}(\alpha^{-3/2}). \tag{5.43}$$

6 Comparison with numerics

To compare with the analytic formula at large α, we solved eq. (A.1) with the Newton-Raphson method for $n = 2, \ldots, 6$ using the following two grids

$$X := \frac{r_0^n}{r^n} \tag{6.1}$$

or

$$\widetilde{X} := \frac{2(\delta-1)^2 (r/r_0)^n}{\delta(1+\delta)(r/r_0)^{2n} + (\delta^2 - 8\delta + 3)(r/r_0)^n + 3\delta - 1}, \quad \delta := \left(2 + 0.2 \left(\frac{n\alpha}{n-1}\right)^{\frac{2n}{n+2}}\right)^{-1}. \tag{6.2}$$

The former is used for the $n = 2$ case and for small value of α in other dimensions ($n = 3, 4, 5, 6$). For $n > 2$, the latter is used to keep the resolution around the transition region at large α. We used $100, 200, 400$ or 800 meshes with the fourth order difference scheme, so that the Smarr formula (A.4) satisfies enough accuracy.

In the figure 2, the metric functions for $n = 4$ are presented. The metric approaches to that of the pure GB black strings at large α. The appearance of the transition region is clearer if we take a look on the quantity $r^{n+1} r_0^{-n} a'(r) \propto a'(X)$ (figure 3).

In figures 4–6, physical quantities of EGB black strings are compared with the large α results. Other than the relative tension, each quantities are normalized by the GR values (C.11). As a characteristic behavior, one can notice that the relative tension once falls to a minimum before it gradually grows to the large α limit.[3] Because of the slow convergence due to the fractional power $\alpha^{-\frac{n-2}{n+2}}$ in the correction, it is difficult to see the behavior at $\alpha \to \infty$ in eqs. (5.25), (5.27), (5.29) and (5.30), directly. Instead, we use the

[3]The same behavior has already been observed in $d = 6, 8$ ($n = 2, 4$) (See figure 5 in ref. [18]).

JHEP09(2022)135

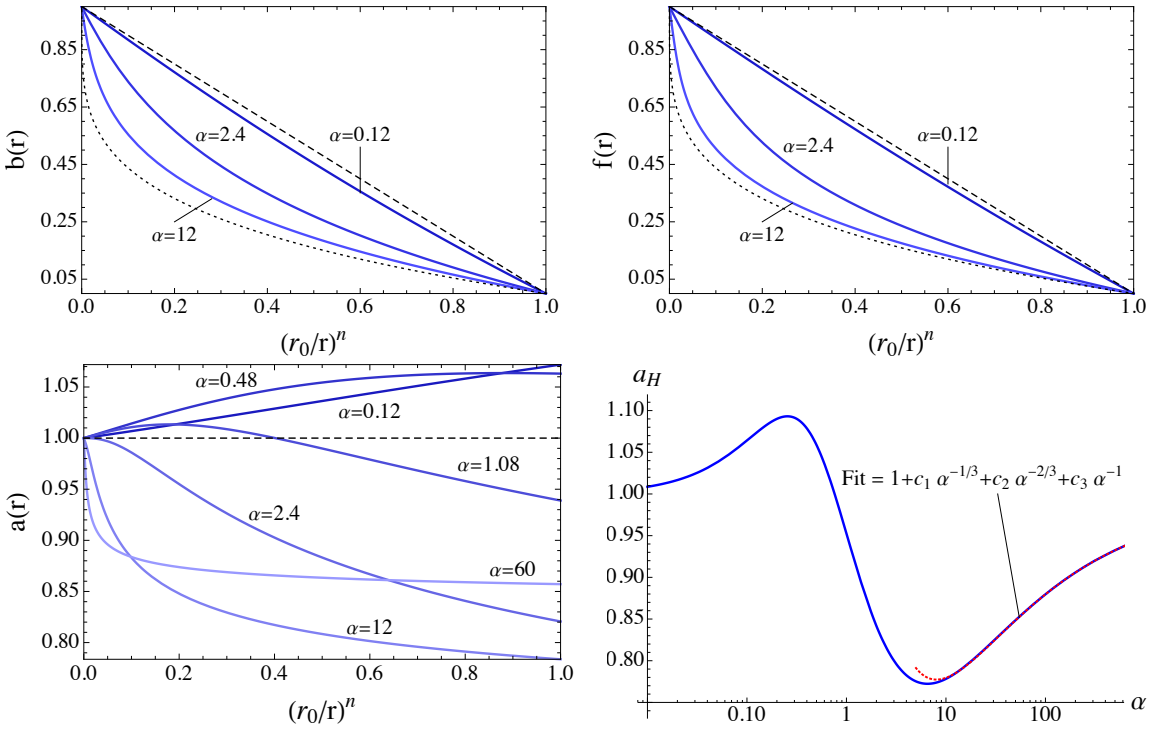

Figure 2. Metric functions in $n = 4$ ($d = 8$). GR and pure GB black strings correspond to the black dashed and dotted curves respectively. $a_H = a(r_0)$ admits an oscillatory behavior as a function of α, which eventually goes back to $a_H = 1$ in $\mathcal{O}(\alpha^{-\frac{n-2}{n+2}})$. The red dotted curve is a fit curve.

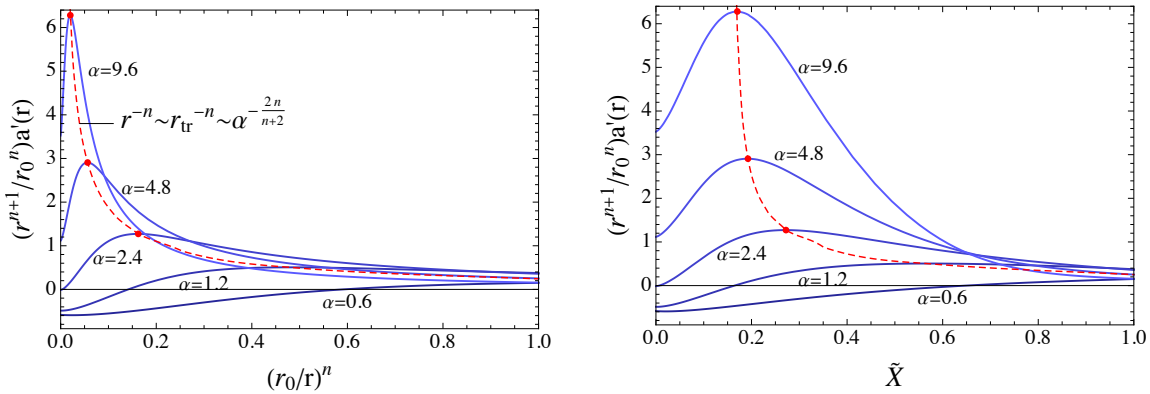

Figure 3. Appearance of the transition scale $r_{\rm tr}$ in the metric function. The red dashed curves are the peak position for each α. In the right panel, one can see that another coordinate $\widetilde{X}$ keeps the transition region in the center area for better resolution at larger α.

JHEP09(2022)135

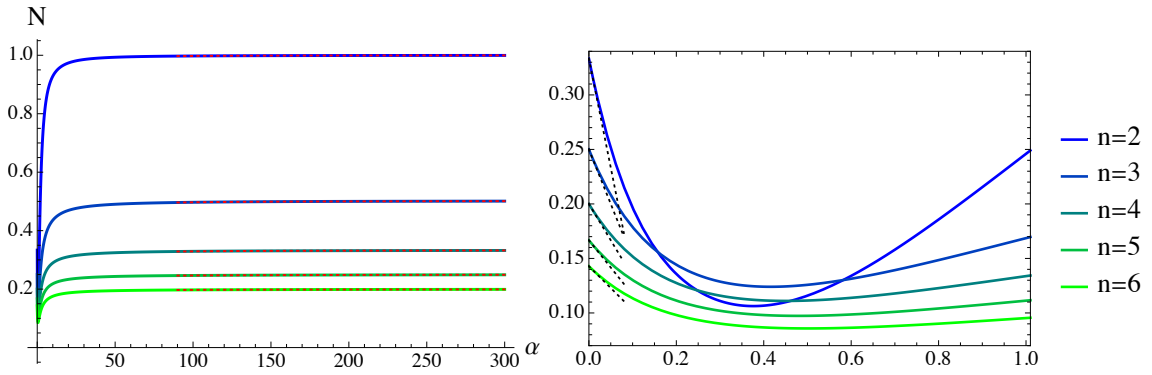

Figure 4. Relative tension vs. α. Numerical results are plotted by solid curves for each dimension. Red dotted curves are the fitting curves in eq. (6.3) for $n > 2$ and eq. (6.7) for $n = 2$. The right panel is a closeup of the small parameter region. Black dotted curves are the linear approximation (C.12).

following fitting curves to compare with the numerical result

$$N = \frac{1}{n-1}\left(1 + \sum_{i=1} c_i \alpha^{-i\frac{n-2}{n+2}}\right), \tag{6.3}$$

$$\frac{M}{M_{\rm GR}} = \alpha\left(1 + \sum_{i=1} c_i \alpha^{-i\frac{n-2}{n+2}}\right), \tag{6.4}$$

$$\frac{T_{\rm H}}{T_{\rm H,GR}} = \frac{n-2}{2n}\left(1 + \sum_{i=1} c_i \alpha^{-i\frac{n-2}{n+2}}\right), \tag{6.5}$$

$$\frac{S}{S_{\rm GR}} = \frac{2(n+1)}{n-1}\alpha\left(1 + \sum_{i=1} c_i \alpha^{-i\frac{n-2}{n+2}}\right), \tag{6.6}$$

where we include correction terms up to $\mathcal{O}(\alpha^{-1})$. The above estimates are only for $n > 2$. For $n = 2$, reflecting the results (5.42) and (5.43), we rather fit by

$$N = 1 - c\,\alpha^{-3/2}, \quad M = c\,\alpha, \quad S = c\sqrt{\alpha}, \quad T_{\rm H} = \frac{c}{\alpha}. \tag{6.7}$$

We find that all these fittings match the numerical results well at the large α region.

7 Extension to Einstein-Lovelock black holes

So far, we have investigated the large α limit in the EGB theory. Here, we discuss the possible extension to the Einstein-Lovelock theories [8] whose action is given by[4]

$$S = \frac{1}{16\pi G}\int dx^d \sqrt{-g}\left(R + \sum_{k=2}^{\lfloor (d-1)/2 \rfloor} \alpha'_k \mathcal{L}_k\right), \tag{7.1}$$

[4]For simplicity, we only consider the asymptotically flat background. However, we expect other non-flat backgrounds such as (A)dS or squashed Kaluza-Klein also admit the similar simplification as long as the typical scale of the background is sufficiently larger than the transition scale.

JHEP09(2022)135

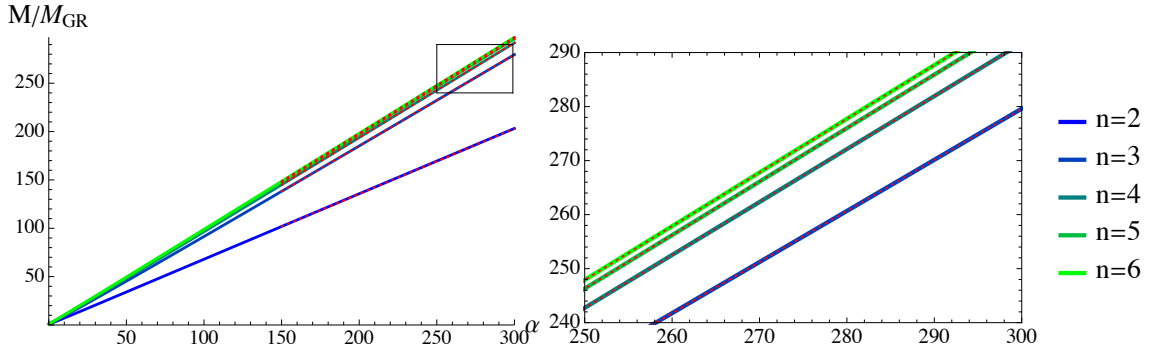

Figure 5. Mass vs. α. Numerical results are plotted by solid curves for each dimension. Red dotted curves are the fitting curves in eq. (6.4) for $n > 2$ and eq. (6.7) for $n = 2$.

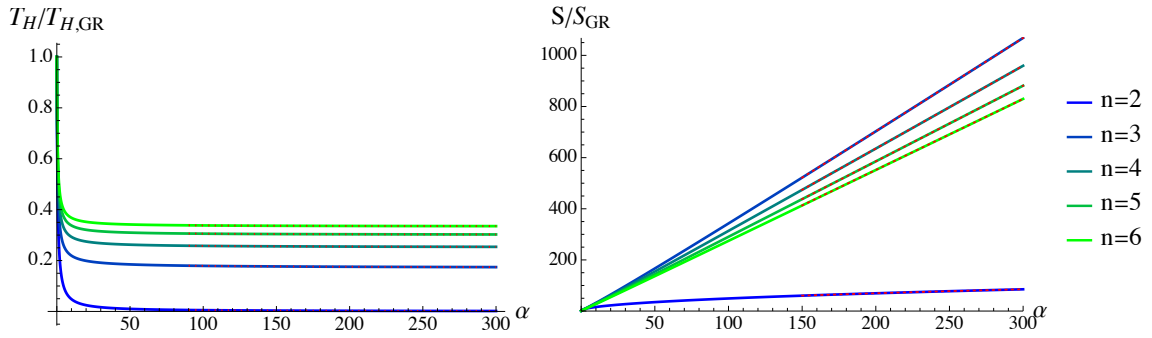

Figure 6. Temperature and entropy vs. α. Numerical results are plotted by solid curves for each dimension. Red dotted curves are the fitting curves in eqs. (6.5) and (6.6) for $n > 2$ and eq. (6.7) for $n = 2$.

where the k th Lovelock term $\mathcal{L}_k$ is given by

$$\mathcal{L}_k := 2^{-k}\delta^{a_1b_1\cdots a_kb_k}_{c_1d_1\cdots c_kd_k}R^{c_1d_1}{}_{a_1b_1}\cdots R^{c_kd_k}{}_{a_kb_k}. \tag{7.2}$$

In $d = n+3$ dimension, the static black hole solution can be obtained by the ansatz [35, 36]

$$ds^2 = -(1 - r^2\psi(r))dt^2 + \frac{dr^2}{1 - r^2\psi(r)} + r^2 d\Omega^2_{n+1}, \tag{7.3}$$

where $\psi(r)$ is given by the real root of the following polynomial

$$\frac{m_0}{r^{n+2}} = \psi + \sum_{k=2}^{\lfloor n/2+1\rfloor}\alpha_k\psi^k, \quad \alpha_k := \alpha'_k\prod_{\ell=3}^{2k}(n+3-\ell). \tag{7.4}$$

The mass parameter m_0 is determined by

$$m_0 = r_0^n\left(1 + \sum_{k=2}^{\lfloor n/2+1\rfloor}\widehat{\alpha}_k\right), \quad \widehat{\alpha}_k := r_0^{-2(k-1)}\alpha_k, \tag{7.5}$$

JHEP09(2022)135

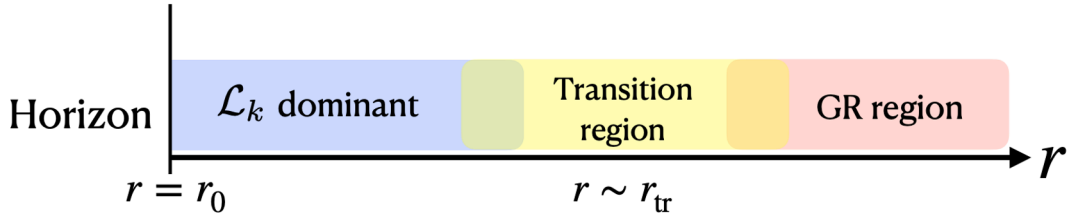

Figure 7. Separate regions in the Einstein-Lovelock black hole with a correction $\mathcal{L}_k$ for $\widehat{\alpha}_k \gg 1$.

where $\psi(r_0) = r_0^{-2}$, and $r = r_0$ is the horizon radius. With the normalized metric function $\widehat{\psi} := r_0^2\psi$, the condition (7.4) is rewritten in the dimensionless form

$$0 = \widehat{\psi} - \left(\frac{r_0}{r}\right)^{n+2} + \sum_{k=2}^{\lfloor n/2+1 \rfloor} \widehat{\alpha}_k \left(\widehat{\psi}^k - \left(\frac{r_0}{r}\right)^{n+2}\right). \tag{7.6}$$

If the k-th order is exclusively dominant, the solution becomes that of pure k-th Lovelock theory [37]

$$\widehat{\psi} \simeq \left(\frac{r_0}{r}\right)^{\frac{n+2}{k}} \quad \Rightarrow \quad g_{tt} \simeq -1 + \left(\frac{r_0}{r}\right)^{\frac{n-2k+2}{k}}. \tag{7.7}$$

7.1 With a $\mathcal{L}_k$

First, we examine whether the similar separation of scales occurs in the Einstein-Lovelock theory with a single Lovelock term $\mathcal{L}_k$ by assuming $\widehat{\alpha}_k \gg 1$. It is obvious that the Lovelock term becomes dominant around the horizon where the metric almost becomes the pure Lovelock solution (7.7), while the post-Minkowski behavior is obtained at large r. In the intermediate region if it exists, the following terms should be comparable in eq. (7.4)

$$\widehat{\psi} \sim \widehat{\alpha}_k \widehat{\psi}^k \sim \widehat{\alpha}_k \left(\frac{r_0}{r}\right)^{n+2}, \tag{7.8}$$

which determines a transition scale

$$r \sim r_{\rm tr} := r_0\, \widehat{\alpha}_k{}^{\frac{k}{(k-1)(n+2)}}. \tag{7.9}$$

Therefore, the Einstein-Lovelock theory with a single Lovelock term can admits the similar structure as in the EGB theory (see figure 7). One can check that the transition scale in the EGB theory (3.6) is reproduced by setting $k = 2$.

7.2 With $\mathcal{L}_2$ and $\mathcal{L}_3$

Next, we consider more general cases in which the theory includes multiple Lovelock corrections. For instance we focus on the Einstein-Lovelock theory only with the second order and third order Lovelock terms, whose normalized coupling constants are large:

$$1 \ll \widehat{\alpha}_2, \widehat{\alpha}_3. \tag{7.10}$$

JHEP09(2022)135

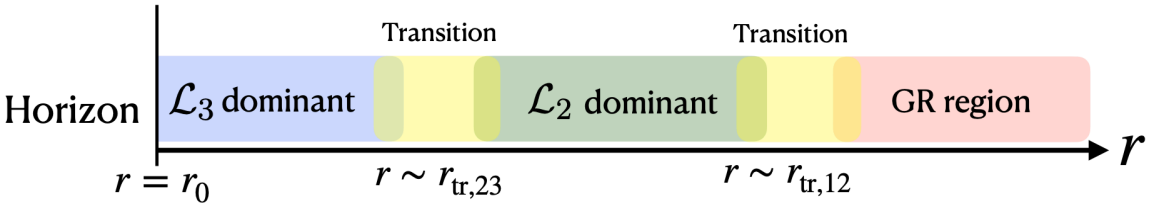

Figure 8. Three separate regions in the Einstein-Lovelock black hole with $\mathcal{L}_2$ and $\mathcal{L}_3$ corrections for $1 \ll \widehat{\alpha}_2 \ll \widehat{\alpha}_3 \ll \widehat{\alpha}_2^2$.

.

Here we do not assume the hierarchy between the two. Then, the transition between the $\mathcal{L}_3$-dominant and $\mathcal{L}_2$-dominant regions can exist if the following terms become comparable in eq. (7.4)

$$\widehat{\alpha}_2\widehat{\psi}^2 \sim \widehat{\alpha}_3\widehat{\psi}^3 \sim (\widehat{\alpha}_2 + \widehat{\alpha}_3)\left(\frac{r_0}{r}\right)^{n+2}, \tag{7.11}$$

which gives a transition scale

$$r \sim r_{\rm tr,23} := r_0\left(\widehat{\alpha}_3^2(\widehat{\alpha}_2 + \widehat{\alpha}_3)/\widehat{\alpha}_2^3\right)^{\frac{1}{n+2}}. \tag{7.12}$$

Similarly, the transition between $\mathcal{L}_2$ dominant and GR region would occur if

$$\widehat{\psi} \sim \widehat{\alpha}_2\widehat{\psi}^2 \sim (\widehat{\alpha}_2 + \widehat{\alpha}_3)\left(\frac{r_0}{r}\right)^{n+2}. \tag{7.13}$$

This introduces another transition scale

$$r \sim r_{\rm tr,12} := r_0\left(\widehat{\alpha}_2(\widehat{\alpha}_2 + \widehat{\alpha}_3)\right)^{\frac{1}{n+2}}. \tag{7.14}$$

To obtain the separation of scales $r_0 \ll r_{\rm tr,23} \ll r_{\rm tr,12}$, we also require

$$\frac{r_{\rm tr,12}}{r_{\rm tr,23}} \sim \left(\frac{\widehat{\alpha}_2^2}{\widehat{\alpha}_3}\right)^{\frac{2}{n+2}} \gg 1, \quad \frac{r_{\rm tr,23}}{r_0} = \left(\frac{\widehat{\alpha}_3^2}{\widehat{\alpha}_2^2} + \frac{\widehat{\alpha}_3^3}{\widehat{\alpha}_2^3}\right)^{\frac{1}{n+2}} \gg 1, \tag{7.15}$$

which is equivalent to

$$\widehat{\alpha}_2 \ll \widehat{\alpha}_3 \ll \widehat{\alpha}_2^2. \tag{7.16}$$

This introduces an additional hierachy between $\widehat{\alpha}_2$ and $\widehat{\alpha}_3$. With the latter condition, one can check that the discarded terms in eq. (7.4) becomes negligible at each transition scale

$$\left.\frac{\widehat{\psi}}{\widehat{\alpha}_2\widehat{\psi}^2}\right|_{r=r_{\rm tr,23}} \sim \frac{\widehat{\alpha}_3}{\widehat{\alpha}_2^2} \ll 1, \quad \left.\frac{\widehat{\alpha}_3\widehat{\psi}^3}{\widehat{\alpha}_2\widehat{\psi}^2}\right|_{r=r_{\rm tr,12}} \sim \frac{\widehat{\alpha}_3}{\widehat{\alpha}_2^2} \ll 1. \tag{7.17}$$

Therefore, we conclude that, at the large coupling limit, multiple Lovelock terms lead to the layered structure in which each Lovelock term becomes dominant one by one through the multiple transition regions (figure 8). Note that the $\mathcal{L}_2$-dominant region cannot appear inside the $\mathcal{L}_3$-dominant region, as it requires two contradicting conditions $\widehat{\alpha}_3 \ll \widehat{\alpha}_2^2$ and $\widehat{\alpha}_3 \gg \widehat{\alpha}_2^2$.

JHEP09(2022)135

8 Summary

In this article, we have constructed the analytic solutions of black strings in the $d = n + 4$ EGB theory, using the novel method of the large α approximation, where α is defined as the dimensionless GB coupling constant normalized by the horizon radius. The points of this method are summarized as follows:

- For sufficiently large α, *the GB region*, where the GB correction is dominant over the Einstein-Hilbert term, appears near the horizon. In the GB region, the black string metric can be obtained analytically by expanding in $1/\alpha$.
- Since the spacetime is asymptotically flat in the transverse direction to the horizon, the GB correction ceases to be dominant at large enough distance from the horizon where we also have *the GR region* in which the metric is approximated as the post-Minkowski spacetime of GR.
- There is the transition region between the two regions at the scale $r_{\rm tr} = r_0\, \alpha^{\frac{2}{n+2}}$ at large α.
- These three regions admit overlaps at large α, and hence the entire geometry can be obtained by the matched asymptotic expansion.

Using this method, we have obtained the analytic solutions of black strings, from which we have also obtained the phase diagram of the EGB black string analytically for large α. By solving the EGB equations numerically using the Newton-Raphson method for $n = 2, \ldots, 6$, we have shown that the resulting phase diagram is consistent with the analytic formula obtained by the large α approach. Lastly, we have discussed possible extensions to Einstein-Lovelock theories.

This work has several possibilities of development. A quick application will be the extension to the Einstein-Lovelock black strings with a single or multiple Lovelock terms. As seen in the last section, the analysis with a single Lovelock correction will be almost parallel to the EGB theory. For the theories with more than one Lovelock terms, one has to solve multiple layers around the horizon in which each Lovelock term becomes dominant in turn. It would be also interesting if one can apply to more realistic cases such as quantum corrected black holes in M-theory [38].

The application to a rotating black hole in the EGB theory or Einstein-Lovelock theories is a challenging but fruitful project, since an exact solution of such a black hole is not yet found in the higher curvature theory (see ref. [25] on a rotating EGB black hole at large d). If we intend to construct an analytic solution of a rotating black hole at large α, we first have to obtain the rotating black hole solutions in the pure GB theory or pure Lovelock theory. This deserves our future work.

We should note that spacetimes in Einstein-Lovelock theories generically suffer from pathologies in the strong field regime, such as short scale instabilities [39], shockwave formation [40], and more remarkably the loss of hyperbolicity [41–43]. Nevertheless, it is not clear whether or not every solution obtained by our approach is in this pathological regime.

JHEP09(2022)135

For example, it is shown that static EGB black holes admit such instabilities and the loss of hyperbolicity at large α only in $d = 5, 6$ [39, 41], that correspond to the transverse section of $d = 6, 7$ black strings. This might imply that, in higher dimensions, those pathologies become milder outside the horizon.

Lastly, we would also like to point out the possibility of more general and sophisticated formulation. The large d limit [22] which is another successful approximation, has lead to the effective theory approach [44] or equivalent membrane paradigm [45], that greatly simplified the analysis. If one can find an effective description in the large α approximation, that may enhance the understandings and broaden the applicability of this approximation.

Acknowledgments

We thank Harvey S. Reall and Norihiro Tanahashi for useful comments and discussions on the well-posedness in Lovelock theories. This work is supported by Toyota Technological Institute Fund for Research Promotion A. RS was supported by JSPS KAKENHI Grant Number JP18K13541. ST was supported by JSPS KAKENHI Grant Number 21K03560.

A Equations

Here we present the explicit form of the field equation

$$\mathcal{E}_{\mu\nu} = R_{\mu\nu} - \frac{1}{2}Rg_{\mu\nu} + \alpha_{\rm GB}H_{\mu\nu}.$$

$\mathcal{E}_{tt}$

$$\begin{aligned}0 =& \frac{n(n+1)a(r)(f(r)-1)}{f(r)} + rf'(r)\left(\frac{ra'(r)}{2f(r)} + \frac{(n+1)a(r)}{f(r)}\right) + (n+1)ra'(r) - \frac{r^2a'(r)^2}{2a(r)} + r^2a''(r) \\ &+ \frac{n(n+1)\alpha_{\rm GB}}{r^2}\left(\frac{(f(r)-1)r^2(a'(r)^2 - 2a(r)a''(r))}{a(r)} - \frac{(n-1)(n-2)a(r)(f(r)-1)^2}{f(r)}\right. \\ &\left. - \frac{(3f(r)-1)r^2f'(r)a'(r)}{f(r)} - \frac{2(n-1)(f(r)-1)r(a(r)f'(r)+a'(r)f(r))}{f(r)}\right).\end{aligned} \tag{A.1a}$$

$\mathcal{E}_{zz}$

$$\begin{aligned}0 =& \frac{n(n+1)b(r)(f(r)-1)}{f(r)} + rf'(r)\left(\frac{rb'(r)}{2f(r)} + \frac{(n+1)b(r)}{f(r)}\right) + (n+1)rb'(r) - \frac{r^2b'(r)^2}{2b(r)} + r^2b''(r) \\ &+ \frac{n(n+1)\alpha_{\rm GB}}{r^2}\left(\frac{(f(r)-1)r^2(b'(r)^2 - 2b''(r))}{b(r)} - \frac{(n-1)(n-2)b(r)(f(r)-1)^2}{f(r)}\right. \\ &\left. - \frac{(3f(r)-1)r^2f'(r)a'(r)}{f(r)} - \frac{2(n-1)(f(r)-1)r(b(r)f'(r)+b'(r)f(r))}{f(r)}\right).\end{aligned} \tag{A.1b}$$

JHEP09(2022)135

$\boldsymbol{\mathcal{E}_{rr}}$

$$0=-\frac{r^2a'(r)b'(r)}{4a(r)b(r)}-\frac{(n+1)ra'(r)}{2a(r)}-\frac{(n+1)rb'(r)}{2b(r)}-\frac{n(n+1)(f(r)-1)}{2f(r)}$$
$$+\frac{n(n+1)\alpha_{\rm GB}}{r^2}\left(\frac{(3f(r)-1)r^2a'(r)b'(r)}{2a(r)b(r)}+(n-1)(f(r)-1)r\left(\frac{a'(r)}{a(r)}+\frac{b'(r)}{b(r)}\right)\right.$$
$$\left.+\frac{(n-2)(n-1)(f(r)-1)^2}{2f(r)}\right) \tag{A.1c}$$

$\boldsymbol{\mathcal{E}^t{}_t+\mathcal{E}^z{}_z-\mathcal{E}_\Omega}$

$$0=\frac{ra'(r)}{a(r)}-\frac{r^2a'(r)b'(r)}{2a(r)b(r)}+\frac{rb'(r)}{b(r)}+\frac{(n+2)rf'(r)}{f(r)}+\frac{n(n+3)(f(r)-1)}{f(r)}$$
$$+\frac{\alpha_{\rm GB}}{r^2}\left[\frac{3nr^3f'(r)a'(r)b'(r)}{a(r)b(r)}+\frac{2nr^2f'(r)(1-3f(r))}{f(r)}\left(\frac{a'(r)}{a(r)}+\frac{b'(r)}{b(r)}\right)-\frac{n(n-1)(n-2)(n+5)(f(r)-1)^2}{f(r)}\right.$$
$$-\frac{nr^3f(r)a'(r)b'(r)}{a(r)b(r)}\left(\frac{a'(r)}{a(r)}+\frac{b'(r)}{b(r)}\right)+\frac{(n-1)n(3f(r)-1)r^2a'(r)b'(r)}{a(r)b(r)}+\frac{2nf(r)r^3(a''(r)b'(r)+a'(r)b''(r))}{a(r)b(r)}$$
$$\left.+2n(f(r)-1)r^2\left(\frac{a'(r)^2}{a(r)^2}+\frac{b'(r)^2}{b(r)^2}-\frac{3(n-1)}{r}\left(\frac{a'(r)}{a(r)}+\frac{b'(r)}{b(r)}\right)-\frac{2a''(r)}{a(r)}-\frac{2b''(r)}{b(r)}-\frac{(n-1)(n+4)f'(r)}{rf(r)}\right)\right] \tag{A.1d}$$

As shown in ref. [18], the following combinations are integrable

$$R^t{}_t+\alpha\left(H^t{}_t+\frac{1}{2}\mathcal{L}_{\rm GB}\right)=\frac{1}{r^{n+1}}\sqrt{\frac{f}{ab}}\frac{d}{dr}\left[\frac{r^{n+1}b'}{2}\sqrt{\frac{af}{b}}\left(-1+\frac{2(n+1)\alpha_{\rm GB}}{r^2}\left(n(f-1)+\frac{rfa'}{a}\right)\right)\right]. \tag{A.2}$$

$$R^z{}_z+\alpha\left(H^z{}_z+\frac{1}{2}\mathcal{L}_{\rm GB}\right)=\frac{1}{r^{n+1}}\sqrt{\frac{f}{ab}}\frac{d}{dr}\left[\frac{r^{n+1}a'}{2}\sqrt{\frac{bf}{a}}\left(-1+\frac{2(n+1)\alpha_{\rm GB}}{r^2}\left(n(f-1)+\frac{rfb'}{b}\right)\right)\right]. \tag{A.3}$$

Thus, the condition $R^t{}_t-R^z{}_z+\alpha(H^t{}_t-H^z{}_z)=0$ leads to the Smarr-type formula

$$M=\mathcal{T}L+T_{\rm H}S. \tag{A.4}$$

A.1 $1/\alpha$ expansion

We define the dimensionless coupling constant α with the horizon radius r_0 as in eq. (3.3). The equation for the $1/\alpha$ correction to the pure GB solution (4.2) is given by the combination of eq. (A.1) expanded in $1/\alpha$

$$\left(\frac{r}{r_0}\right)^{\frac{n+2}{2}}\left(\frac{f(r)}{n(n+1)}\times\ (A.1a)+\frac{2}{n(n+1)(n+2)}\times\ (A.1b)\right.$$
$$\left.-\frac{2f(r)}{n(n+1)(n+2)}\times\ (A.1c)-\frac{f(r)}{n(n+2)}\times\ (A.1d)\right)$$
$$=\left(1-\left(\frac{r_0}{r}\right)^{\frac{n-2}{2}}\right)r^2a_1''(r)+\left(\frac{n}{2}-\left(\frac{r_0}{r}\right)^{\frac{n-2}{2}}\right)ra_1'(r)-\frac{n+4}{2n^2+2n}\frac{r^2}{r_0^2}+\mathcal{O}(\alpha^{-1}), \tag{A.5}$$

JHEP09(2022)135

and

$$\frac{r^{n-1}}{r_0^n}\left(-2f(r)\times\ (A.1a)-\frac{8}{n+2}\times\ (A.1b)+\frac{8f(r)}{n+2}\times\ (A.1c)+\frac{4(n+1)f(r)}{n+2}\times\ (A.1d)\right)$$
$$=\frac{d}{dr}\left[n(n+1)(2-n)a_1(r)+4n(n^2-1)\left(\frac{r}{r_0}\right)^{\frac{n-2}{2}}f_1(r)-\frac{2(n-2)(n+3)}{n+2}\left(\frac{r}{r_0}\right)^{\frac{n+2}{2}}\right]$$
$$+\mathcal{O}(\alpha^{-1}), \tag{A.6}$$

which lead to eqs. (4.3) and (4.5), respectively. The expansion of eq. (A.1c) also leads to eq. (4.4).

B An integration in $1/\alpha$ expansion

Here we study the asymptotic behavior around $x=0$ ($r\gg r_0$) of the integration (4.7), which is rewritten as

$$\mathsf{F}_n(x):=\int_x^1\frac{y^{\frac{n+2}{2-n}}-1}{1-y}dy \tag{B.1}$$
$$=I_n(x)+(n-2)\left[\frac{x^{4-\frac{4}{n-2}}-1}{4(n-3)}+\frac{x^{3-\frac{4}{n-2}}-1}{3n-10}+\frac{x^{2-\frac{4}{n-2}}-1}{2(n-4)}+\frac{x^{1-\frac{4}{n-2}}-1}{n-6}+\frac{x^{-\frac{4}{n-2}}-1}{4}\right], \tag{B.2}$$

where we defined a finite function $I_n(x)$ for $n>2$ by the following integral

$$I_3(x)=0,\quad I_n(x):=\int_x^1\frac{1-y^{\frac{4(n-3)}{n-2}}}{1-y}dy\quad(n>3). \tag{B.3}$$

The integration formula

$$\int_0^1\frac{1-x^{\mu-1}}{1-x}dx=H_{\mu-1}\quad(\mathrm{Re}(\mu)>0) \tag{B.4}$$

guarantees that this function takes a finite value at $x=0$

$$I_n(0)=H_{\frac{4(n-3)}{n-2}}, \tag{B.5}$$

where H_μ is the Harmonic number, whose noninteger values are defined by the digamma function and the Euler constant $H_\mu:=\psi(\mu+1)+\gamma$. For $n=3,4,6$ cases, although the expression (B.2) seems singular, one can obtain the regular expression by taking the continuous limit $n\to3,4,6$, which leads to $\ln x\propto\ln r$ behavior for $r\gg r_0$. The dominant behavior in $\mathsf{F}_n(x)$ for $x\ll1$ becomes

$$\mathsf{F}_n(x)\simeq\frac{n-2}{4}x^{-\frac{4}{n-2}}\quad(x\ll1), \tag{B.6}$$

which gives the asymptotic behavior for $r\gg r_0$

$$\mathsf{F}_n\left((r_0/r)^{\frac{n-2}{2}}\right)\simeq\frac{n-2}{4}\frac{r^2}{r_0^2}. \tag{B.7}$$

JHEP09(2022)135

C Linear perturbation from GR at small $\alpha_{\rm GB}$

Here we extend the small $\alpha_{\rm GB}$ analysis of the black string in ref. [18] to the arbitrary dimension. Let us consider $\mathcal{O}(\alpha_{\rm GB})$ correction to the GR black string solution

$$a = 1 + \frac{\alpha_{\rm GB}}{r_0^2}\,\tilde{a}_1, \quad b = 1 - \frac{r_0^n}{r^n} + \frac{\alpha_{\rm GB}}{r_0^2}\,\tilde{b}_1, \quad f = 1 - \frac{r_0^n}{r^n} + \frac{\alpha_{\rm GB}}{r_0^2}\,\tilde{f}_1. \tag{C.1}$$

The linear perturbation is solved as

$$\tilde{a}_1 = -\frac{n+1}{n+2}\left[\frac{n r_0^{2n+2}}{r^{2n+2}}\,{}_2F_1\left(1,2+\frac{2}{n},3+\frac{2}{n};\frac{r_0^n}{r^n}\right) - 2(n+1)\log\left(1-\frac{r_0^n}{r^n}\right)\right], \tag{C.2}$$

$$\begin{aligned}
\tilde{b}_1 =& -\frac{n(n+1)H_{\frac{n+2}{n}} + n(n^2+n-2)}{n+2}\frac{r_0^n}{r^n} + \left(\frac{2(n+1)}{n+2} - (n+1)\frac{r_0^n}{r^n}\right)\log\left(1-\frac{r_0^n}{r^n}\right) \\
&+ (n^2+n-1)\frac{r_0^{2n+2}}{r^{2n+2}}\left[\frac{2(n+1)\,{}_2F_1\left(2,\frac{n+2}{n},2+\frac{2}{n};\frac{r_0^n}{r^n}\right)}{n+2} - 1\right] \\
&+ \frac{r_0^{3n+2}}{r^{3n+2}}\left[\frac{n(3n+4)(n+1)\,{}_2F_1\left(1,3+\frac{2}{n},4+\frac{2}{n};\frac{r_0^n}{r^n}\right)}{(3n+2)(n+2)} - \frac{\left(4n^3+15n^2+8n-8\right)\,{}_2F_1\left(2,2+\frac{2}{n},3+\frac{2}{n};\frac{r_0^n}{r^n}\right)}{2(n+2)}\right] \\
&+ \frac{r_0^{4n+2}}{r^{4n+2}}\left[\frac{2\left(n^3+3n^2+n-1\right)\,{}_2F_1\left(2,3+\frac{2}{n},4+\frac{2}{n};\frac{r_0^n}{r^n}\right)}{3n+2} + \frac{n^2(n+1)\,{}_2F_1\left(2,4+\frac{2}{n},5+\frac{2}{n};\frac{r_0^n}{r^n}\right)}{2(n+2)(2n+1)}\right]
\end{aligned} \tag{C.3}$$

and

$$\begin{aligned}
\tilde{f}_1 =& -\frac{n r_0^n}{r^n}\left[\frac{(n+1)H_{\frac{n+2}{n}} + n^2 - n - 4}{n+2} - \frac{(n+1)\log\left(1-\frac{r_0^n}{r^n}\right)}{n+2}\right] \\
&+ \frac{r_0^{2n+2}}{r^{2n+2}}\frac{\left(2(n+1)(n^2+n-1)\,{}_2F_1\left(2,1+\frac{2}{n},2+\frac{2}{n};\frac{r_0^n}{r^n}\right) - n^3 - 5n^2 - 4n + 2\right)}{n+2} \\
&- \frac{r_0^{3n+2}}{r^{3n+2}}\left[\frac{\left(4n^3+15n^2+8n-8\right)\,{}_2F_1\left(2,2+\frac{2}{n},3+\frac{2}{n};\frac{r_0^n}{r^n}\right)}{2(n+2)} - n\right] \\
&+ \frac{n+1}{3n+2}\frac{r_0^{4n+2}}{r^{4n+2}}\left[\frac{n(3n+4)\,{}_2F_1\left(1,3+\frac{2}{n},4+\frac{2}{n};\frac{r_0^n}{r^n}\right)}{n+2} + 2(n^2+2n-1)\,{}_2F_1\left(2,3+\frac{2}{n},4+\frac{2}{n};\frac{r_0^n}{r^n}\right)\right] \\
&+ \frac{n^2(n+1)\,{}_2F_1\left(2,4+\frac{2}{n},5+\frac{2}{n};\frac{r_0^n}{r^n}\right)}{2(n+2)(2n+1)}\frac{r_0^{5n+2}}{r^{5n+2}},
\end{aligned} \tag{C.4}$$

where H_k is the Harmonic number and ${}_2F_1(a,b,c;x)$ is the hypergeometric function. We imposed the boundary condition as

$$\tilde{a}_1 \to 0, \quad \tilde{b}_1 \to 0, \quad \tilde{f}_1 \to 0, \quad (r \to \infty), \tag{C.5}$$

$$\tilde{a}_1 \to \mathcal{O}(1), \quad \tilde{b}_1 \to \mathcal{O}(r-r_0), \quad \tilde{f}_1 \to \mathcal{O}(r-r_0), \quad (r \to r_0). \tag{C.6}$$

JHEP09(2022)135

Up to the linear order, the thermodynamic variables are obtained as

$$\frac{M}{M_{\rm GR}} = 1 + \left(\frac{n(n+1) H_{\frac{n+2}{n}}}{n+2} + n(n-1) \right) \frac{\alpha_{\rm GB}}{r_0^2} \tag{C.7}$$

$$\frac{\tau}{\tau_{\rm GR}} = 1 + \left(\frac{n(n+1) H_{\frac{n+2}{n}}}{n+2} - n(n+3) \right) \frac{\alpha_{\rm GB}}{r_0^2} \tag{C.8}$$

$$\frac{T_{\rm H}}{T_{\rm H,GR}} = 1 - \left(\frac{(n+1) H_{\frac{n+2}{n}}}{n+2} + (n+2)(n-1) \right) \frac{\alpha_{\rm GB}}{r_0^2} \tag{C.9}$$

$$\frac{S}{S_{\rm GR}} = 1 + \left(\frac{(n+1)^2 H_{\frac{n+2}{n}}}{n+2} + 2n(n+1) \right) \frac{\alpha_{\rm GB}}{r_0^2} \tag{C.10}$$

where

$$M_{\rm GR} := \frac{(n+1)\Omega_{n+1} L r_0^n}{16\pi G}, \quad \tau_{\rm GR} := \frac{\Omega_{n+1} r_0^n}{16\pi G}, \quad T_{\rm H,GR} := \frac{n}{4\pi r_0}, \quad S_{\rm GR} := \frac{\Omega_{n+1} L r_0^{n+1}}{4G} \tag{C.11}$$

The relative tension is given by

$$N = \frac{1}{n+1} \left(1 - \frac{2n(n+1)\alpha_{\rm GB}}{r_0^2} \right). \tag{C.12}$$

All these are consistent with the result in ref. [18] for $n = 1, \ldots, 4$.

Open Access. This article is distributed under the terms of the Creative Commons Attribution License (CC-BY 4.0), which permits any use, distribution and reproduction in any medium, provided the original author(s) and source are credited. SCOAP^3 supports the goals of the International Year of Basic Sciences for Sustainable Development.

References

[1] A. Strominger and C. Vafa, *Microscopic origin of the Bekenstein-Hawking entropy*, *Phys. Lett. B* **379** (1996) 99 [hep-th/9601029] [INSPIRE].

[2] P.C. Argyres, S. Dimopoulos and J. March-Russell, *Black holes and submillimeter dimensions*, *Phys. Lett. B* **441** (1998) 96 [hep-th/9808138] [INSPIRE].

[3] J.M. Maldacena, *The large N limit of superconformal field theories and supergravity*, *Adv. Theor. Math. Phys.* **2** (1998) 231 [hep-th/9711200] [INSPIRE].

[4] R. Emparan and H.S. Reall, *Black Holes in Higher Dimensions*, *Living Rev. Rel.* **11** (2008) 6 [arXiv:0801.3471] [INSPIRE].

[5] F.R. Tangherlini, *Schwarzschild field in n dimensions and the dimensionality of space problem*, *Nuovo Cim.* **27** (1963) 636 [INSPIRE].

[6] R. Gregory and R. Laflamme, *Black strings and p-branes are unstable*, *Phys. Rev. Lett.* **70** (1993) 2837 [hep-th/9301052] [INSPIRE].

[7] R. Gregory and R. Laflamme, *The instability of charged black strings and p-branes*, *Nucl. Phys. B* **428** (1994) 399 [hep-th/9404071] [INSPIRE].

JHEP09(2022)135

[8] C. Garraffo and G. Giribet, *The Lovelock Black Holes*, *Mod. Phys. Lett. A* **23** (2008) 1801 [arXiv:0805.3575] [INSPIRE].

[9] C. Barcelo, R. Maartens, C.F. Sopuerta and F. Viniegra, *Stacking a 4-D geometry into an Einstein-Gauss-Bonnet bulk*, *Phys. Rev. D* **67** (2003) 064023 [hep-th/0211013] [INSPIRE].

[10] D. Kastor and R.B. Mann, *On black strings and branes in Lovelock gravity*, *JHEP* **04** (2006) 048 [hep-th/0603168] [INSPIRE].

[11] G. Giribet, J. Oliva and R. Troncoso, *Simple compactifications and black p-branes in Gauss-Bonnet and Lovelock theories*, *JHEP* **05** (2006) 007 [hep-th/0603177] [INSPIRE].

[12] A. Cisterna, S. Fuenzalida, M. Lagos and J. Oliva, *Homogeneous black strings in Einstein-Gauss-Bonnet with Horndeski hair and beyond*, *Eur. Phys. J. C* **78** (2018) 982 [arXiv:1810.02798] [INSPIRE].

[13] A. Cisterna, S. Fuenzalida and J. Oliva, *Lovelock black p-branes with fluxes*, *Phys. Rev. D* **101** (2020) 064055 [arXiv:2001.00788] [INSPIRE].

[14] F. Canfora, A. Cisterna, S. Fuenzalida, C. Henríquez-Báez and J. Oliva, *General relativity from Einstein-Gauss-Bonnet gravity*, *Phys. Rev. D* **104** (2021) 044026 [arXiv:2103.09110] [INSPIRE].

[15] A. Cisterna, C. Henríquez-Báez, N. Mora and L. Sanhueza, *Quasitopological electromagnetism: Reissner-Nordström black strings in Einstein and Lovelock gravities*, *Phys. Rev. D* **104** (2021) 064055 [arXiv:2105.04239] [INSPIRE].

[16] A. Cisterna and J. Oliva, *Exact black strings and p-branes in general relativity*, *Class. Quant. Grav.* **35** (2018) 035012 [arXiv:1708.02916] [INSPIRE].

[17] T. Kobayashi and T. Tanaka, *Five-dimensional black strings in Einstein-Gauss-Bonnet gravity*, *Phys. Rev. D* **71** (2005) 084005 [gr-qc/0412139] [INSPIRE].

[18] Y. Brihaye, T. Delsate and E. Radu, *Einstein-Gauss-Bonnet black strings*, *JHEP* **07** (2010) 022 [arXiv:1004.2164] [INSPIRE].

[19] B. Kleihaus, J. Kunz, E. Radu and B. Subagyo, *Spinning black strings in five-dimensional Einstein-Gauss-Bonnet gravity*, *Phys. Lett. B* **713** (2012) 110 [arXiv:1205.1656] [INSPIRE].

[20] L. Ma, Y.-Z. Li and H. Lü, *$D = 5$ rotating black holes in Einstein-Gauss-Bonnet gravity: mass and angular momentum in extremality*, *JHEP* **01** (2021) 201 [arXiv:2009.00015] [INSPIRE].

[21] R. Emparan, R. Suzuki and K. Tanabe, *The large D limit of General Relativity*, *JHEP* **06** (2013) 009 [arXiv:1302.6382] [INSPIRE].

[22] R. Emparan and C.P. Herzog, *Large D limit of Einstein's equations*, *Rev. Mod. Phys.* **92** (2020) 045005 [arXiv:2003.11394] [INSPIRE].

[23] B. Chen, P.-C. Li and C.-Y. Zhang, *Einstein-Gauss-Bonnet Black Strings at Large D*, *JHEP* **10** (2017) 123 [arXiv:1707.09766] [INSPIRE].

[24] B. Chen, P.-C. Li and C.-Y. Zhang, *Einstein-Gauss-Bonnet Black Rings at Large D*, *JHEP* **07** (2018) 067 [arXiv:1805.03345] [INSPIRE].

[25] R. Suzuki and S. Tomizawa, *Rotating black holes at large D in Einstein-Gauss-Bonnet theory*, *Phys. Rev. D* **106** (2022) 024018 [arXiv:2202.12649] [INSPIRE].

[26] A. Giacomini, J. Oliva and A. Vera, *Black Strings in Gauss-Bonnet Theory are Unstable*, *Phys. Rev. D* **91** (2015) 104033 [arXiv:1503.03696] [INSPIRE].

JHEP09(2022)135

[27] R. Suzuki and S. Tomizawa, *Stable bound orbits around static Einstein-Gauss-Bonnet black holes*, *Phys. Rev. D* **105** (2022) 124033 [arXiv:2204.10087] [INSPIRE].

[28] T. Harmark and N.A. Obers, *General definition of gravitational tension*, *JHEP* **05** (2004) 043 [hep-th/0403103] [INSPIRE].

[29] R.M. Wald, *Black hole entropy is the Noether charge*, *Phys. Rev. D* **48** (1993) R3427 [gr-qc/9307038] [INSPIRE].

[30] V. Iyer and R.M. Wald, *Some properties of Noether charge and a proposal for dynamical black hole entropy*, *Phys. Rev. D* **50** (1994) 846 [gr-qc/9403028] [INSPIRE].

[31] D.G. Boulware and S. Deser, *String Generated Gravity Models*, *Phys. Rev. Lett.* **55** (1985) 2656 [INSPIRE].

[32] N. Dadhich, S.G. Ghosh and S. Jhingan, *The Lovelock gravity in the critical spacetime dimension*, *Phys. Lett. B* **711** (2012) 196 [arXiv:1202.4575] [INSPIRE].

[33] D. Kastor, *The Riemann-Lovelock Curvature Tensor*, *Class. Quant. Grav.* **29** (2012) 155007 [arXiv:1202.5287] [INSPIRE].

[34] P. Suranyi, C. Vaz and L.C.R. Wijewardhana, *The fate of black branes in Einstein-Gauss-Bonnet gravity*, *Phys. Rev. D* **79** (2009) 124046 [arXiv:0810.0525] [INSPIRE].

[35] J.T. Wheeler, *Symmetric Solutions to the Maximally Gauss-Bonnet Extended Einstein Equations*, *Nucl. Phys. B* **273** (1986) 732 [INSPIRE].

[36] R.C. Myers and J.Z. Simon, *Black Hole Thermodynamics in Lovelock Gravity*, *Phys. Rev. D* **38** (1988) 2434 [INSPIRE].

[37] J. Crisostomo, R. Troncoso and J. Zanelli, *Black hole scan*, *Phys. Rev. D* **62** (2000) 084013 [hep-th/0003271] [INSPIRE].

[38] Y. Hyakutake, *Quantum Aspects of Black Objects in String Theory*, *JHEP* **01** (2017) 066 [arXiv:1612.01874] [INSPIRE].

[39] R.A. Konoplya and A. Zhidenko, *(In)stability of D-dimensional black holes in Gauss-Bonnet theory*, *Phys. Rev. D* **77** (2008) 104004 [arXiv:0802.0267] [INSPIRE].

[40] H.S. Reall, N. Tanahashi and B. Way, *Shock Formation in Lovelock Theories*, *Phys. Rev. D* **91** (2015) 044013 [arXiv:1409.3874] [INSPIRE].

[41] H. Reall, N. Tanahashi and B. Way, *Causality and Hyperbolicity of Lovelock Theories*, *Class. Quant. Grav.* **31** (2014) 205005 [arXiv:1406.3379] [INSPIRE].

[42] G. Papallo and H.S. Reall, *On the local well-posedness of Lovelock and Horndeski theories*, *Phys. Rev. D* **96** (2017) 044019 [arXiv:1705.04370] [INSPIRE].

[43] A.D. Kovács and H.S. Reall, *Well-posed formulation of Lovelock and Horndeski theories*, *Phys. Rev. D* **101** (2020) 124003 [arXiv:2003.08398] [INSPIRE].

[44] R. Emparan, T. Shiromizu, R. Suzuki, K. Tanabe and T. Tanaka, *Effective theory of Black Holes in the 1/D expansion*, *JHEP* **06** (2015) 159 [arXiv:1504.06489] [INSPIRE].

[45] S. Bhattacharyya, A. De, S. Minwalla, R. Mohan and A. Saha, *A membrane paradigm at large D*, *JHEP* **04** (2016) 076 [arXiv:1504.06613] [INSPIRE].

JHEP09(2022)135